Photoinduced Mo-CN Bond Breakage in Octacyanomolybdate Leading to Spin Triplet Trapping

Xinghui Qi, Sébastien Pillet, Coen de Graaf, Michał Magott, El-Eulmi Bendeif, Philippe Guionneau, Mathieu Rouzières, Valérie Marvaud, Olaf Stefańczyk, Dawid Pinkowicz*, Corine Mathonière*

Abstract: The photoinduced properties of the octacoordinated complex $K_4Mo^{IV}(CN)_8 \cdot 2H_2O$ were studied by theoretical calculations, crystallography, and optical and magnetic measurements. The crystal structure recorded at 10 K after blue light irradiation reveals an heptacoordinated $Mo(CN)_7$ species originating from the light-induced cleavage of one Mo-CN bond, concomitant with the photoinduced formation of a paramagnetic signal. When this complex is heated to 70 K, it returns to its original diamagnetic ground state, demonstrating full reversibility. The photomagnetic properties show a partial conversion into a triplet state possessing significant magnetic anisotropy, which is in agreement with theoretical studies. Inspired by these results, we isolated the new compound $[K(crypt\text{-}222)]_3[Mo^{IV}(CN)_7] \cdot 3CH_3CN$ using a photochemical pathway, confirming that photodissociation leads to a stable heptacyanomolybdate(IV) species in solution.

The remote control of magnetic properties with light is a fascinating topic in materials science. In coordination chemistry, the well-known light-induced magnetic tunability concerns spin crossover of one single metal center (notably Fe^{II})[1] and metal–metal charge transfer (MMCT) in bimetallic cyanido-bridged networks (e.g., $Co/Fe(CN)_6$),[2] usually associated with local contraction/dilatation of the coordination spheres.[2]

Bimetallic octacyanidometallate-based compounds display appealing features in their photoinduced magnetic states, such as high relaxation temperatures, high Curie temperatures, and site-selective switching.[3–6] The optical spectra of some of these systems display MMCT bands, and consequently, the observed photomagnetic behaviors have been interpreted as MMCT. This scenario was confirmed for $Co^{II}/W^{V}(CN)_8$ systems,[7] but for specific $Cu^{II}/Mo^{IV}(CN)_8$ systems, the results of X-ray magnetic circular dichroism revealed a singlet-triplet crossover centered on the Mo^{IV}.[8] Additionally, theoretical calculations have suggested the photoinduced formation of a triplet located on Mo concomitant with the breakage of one Mo-CN bond in $[Mo(CN)_8]^{4-}$.[8c,d]

We selected $K_4Mo^{IV}(CN)_8 \cdot 2H_2O$ (**1**) for an in-depth investigation of its photomagnetic properties. The first photo- magnetic characterization of 1 using UV light was reported in 2000, and a photooxidation from Mo^{4+} to Mo^{5+} was sugges- ted.[4c] Recently, a spin crossover was proposed to interpret the photoinduced magnetism in a $MoZn_2$ complex[9] and in $(H_4cyclam)[Mo^{IV}(CN)_8] \cdot 1.5H_2O$ (cyclam = 1,4,8,11-tetraaza-cyclodecane).[10] In this work, we demonstrate unambiguously that the reversible photomagnetism in **1** is associated not only with a spin change but also with a profound structural modification of the complex.

Complex **1** was synthesized as described previously.[11] We performed theoretical investigations of **1** using the CASSCF/CASPT2 and TD-DFT approaches to determine the excitation energies.[12] The UV/Vis spectra of **1** in solution and in the solid state are nicely reproduced by the calculations (Figure S2 and Table S1 in the Supporting Information). The lower-energy transitions (430 and 360 nm) were assigned to transitions between the singlet state and triplet states, in line with previous calculations.[13] These spin-forbidden transitions are detectable because they gain intensity through spin–orbit coupling (Tables S1 and S3). At higher energy, the observed intense band (240 nm) is probably due to a combination of multiple spin-allowed excitations and charge transfer excitations.

We performed reflectivity measurements of **1** to evaluate its photochromic properties. Upon exposure to specific wavelengths within the 365–455 nm range at 10 K, a new broad absorption around 650 nm appeared, suggesting a modification of the molybdenum electronic configuration. Then, the complex was subjected to 30 min irradiation at 405 nm (i.e., the most efficient wavelength) to obtain the spectrum of the photoexcited state that is stable over time at 10 K. When **1** was heated further, the

[*] X. Qi, Dr. P. Guionneau, Dr. C. Mathonière,
CNRS, Univ. Bordeaux, Bordeaux INP, ICMCB, UMR 5026, F-33600 Pessac (France)
E-mail: corine.mathoniere@icmcb.cnrs.fr
Dr. O. Stefańczyk
Present address : Department of Chemistry, School of Science, The University of Tokyo, 7−3−1 Hongo, Bunkyo-ku, Tokyo 113-0033 (Japan)
Dr. S. Pillet, Dr. E.-E. Bendeif
Université de Lorraine, CNRS, CRM2, Nancy, 54506 Vandoeuvre -les-Nancy (France)
Dr. C. Graaf
Departament de Química Física i Inorgànica, Universitat Rovira i Virgili, Carrer Marcellí Domingo 1, Tarragona (Spain)
and
ICREA, Passeig Lluís Companys 23, Barcelona 08010 (Spain)
Dr. M. Rouzières,
CNRS, Univ. Bordeaux, CRPP, UMR 5031, F-33600 Pessac (France)
Dr. V. Marvaud
Sorbonne Université, IPCM-CNRS-UMR-8232, cc 229,
4 place Jussieu, 75252 Paris Cedex 05 (France)
M. Magott, Dr. D. Pinkowicz
Jagiellonian University, Faculty of Chemistry, Gronostajowa 2, 30-387 Kraków (Poland)
E-mail: dawid.pinkowicz@uj.edu.pl
Supporting information and the ORCID identification number(s) for the author(s) of this article can be found under:
https://doi.org/10.1002/anie.20191452

characteristic band of the photoexcited state began to disappear and vanished completely around 70 K, the temperature at which **1** recovers its initial state (Figures 1 and S3). Based on the above theoretical calculations, the selective 405 nm excitation allows the lower-energy triplet state to be reached. Complementary calculations were performed to obtain the optimized geometry of the triplet state, which shows a geometry change for Mo from octa- to heptacoordination, similarly to what has been computed for $Cu^{II}/Mo^{IV}(CN)_8$ systems.[8c,d]

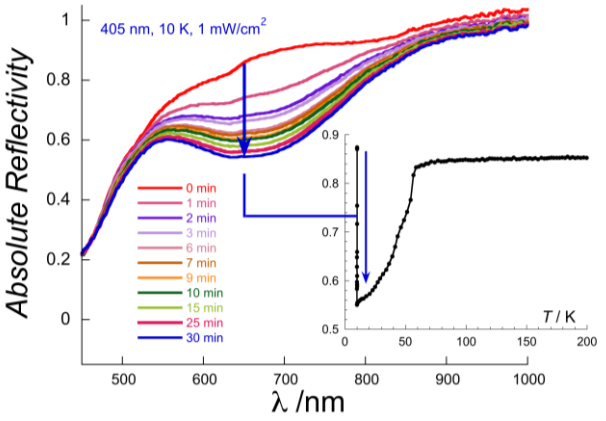

Figure 1. Reflectivity spectra of **1** after 405 nm irradiation for different periods of time (1 mW/cm^2, 10 K). Inset: Temperature dependence of the absolute reflectivity at 650 nm (during (blue arrow) and after excitation in heating mode in the dark (black circles).

To experimentally confirm these drastic light-induced modifications of **1**, single-crystal X-ray diffraction (SXRD) was employed. The crystal structures of the ground state, the photoexcited state, and the relaxed state at 10 K are referred to as **1, 1*** and $\mathbf{1}_{relax}$ respectively. A color change from yellow for **1** to green for **1*** was observed at 10 K upon 30 min exposure to a 405 nm laser (Figure 2b). The green color of **1*** agrees with the appearance of the 650 nm band in the reflectivity spectra. The yellow color of **1** was restored in $\mathbf{1}_{relax}$ by heating **1*** to 70 K.

The good crystallinity allowed us to track the crystal structure variation after light irradiation at 10 K and after thermal relaxation. Selected crystallography data are compiled in Tables S4–S6. At 10 K,the structureof **1** is identical to that reported at room temperature. **1, 1*** and $\mathbf{1}_{relax}$ adopt the same space group *Pnma*, and the global crystal packing is preserved. Compared to **1**, **1*** clearly reveals a cell volume expansion with an increase along the *c* axis. Complex **1*** shows a coexistence of the ground state and the photoexcited state with a partial photoconversion rate of 53%, from which

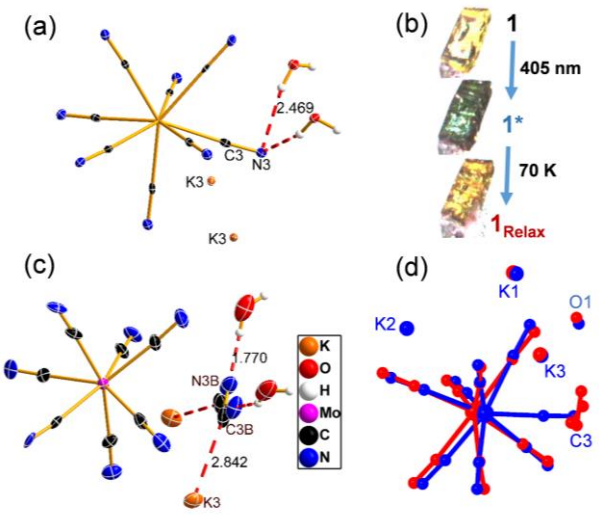

Figure 2. Crystal structures with 70% probability thermal ellipsoids for **1** (a) and $\mathbf{1^*_{PES}}$ c) with hydrogen bonding (red dashed lines). (b) Photographs of crystals of **1**, **1***, and $\mathbf{1}_{relax}$ at 10 K. d) Superposition of relevant fragments for **1** (blue) and $\mathbf{1^*_{PES}}$ (red).[21]

the structure of the photoinduced state has been extracted and is referred to as $\mathbf{1^*_{PES}}$ hereafter.

The comparison of **1, 1*** and $\mathbf{1}_{relax}$ reveals spectacular modifications in the Mo environment. In **1** and $\mathbf{1}_{relax}$, the Mo coordination sphere consists of eight cyanide ligands, afford- ing triangular dodecahedron (TDD) geometry with continuous shape measurement (CShM) values of 0.25 and 0.24, respectively.[14] On the other hand, $\mathbf{1^*_{PES}}$ features a $Mo(CN)_7$ coordination sphere adopting an intermediate geometry between a capped octahedron (COC) and a capped trigonal prism (CTPR), with CshM values of 1.01 and 1.55, respectively.

Figures 2c,d, S4, and S5 show the striking differences in the Mo coordination sphere. In $\mathbf{1^*_{PES}}$, the cleavage of the Mo- C3B bond is confirmed by its drastic elongation from 2.176(3) Å to 3.963(2) Å, indicating that the C3B atom is not linked to the molybdenum center anymore. The C3B-N3B bond length of 1.123(7) Å indicates that the carbon–nitrogen triple bond is preserved. The C3N3 ligand that is sitting on a mirror plane in 1 is significantly shifted out of the mirror plane upon photoexcitation, and is now disordered over two symmetry-related positions. In $\mathbf{1^*_{PES}}$, the Mo center moves in the opposite direction to the broken Mo-CN bond (Figure 2d). The average Mo-C bond length for $\mathbf{1^*_{PES}}$ is 2.153(4) Å, which is slightly shorter than the ones found in **1** (2.161(2) Å). The average Mo-C-N angle slightly changes from 177.5(2) ° in **1** to 176.4(3) ° in $\mathbf{1^*_{PES}}$.

A superposition of the experimental structure of $\mathbf{1^*_{PES}}$ and the calculated structure of $\mathbf{1^*_{PEScal}}$ obtained from periodic DFT calculations shows identical Mo coordination spheres. The only difference comes from the disorder that affects the broken C3B-N3B moiety in $\mathbf{1^*_{PES}}$ (Figure S6), as this disorder originating from the symmetry is not considered in $\mathbf{1^*_{PEScal}}$.

The detached cyanide ligand is trapped by potassium ions and water molecules as shown in Figures 2c and S4b–d. The nitrogen atoms of cyanide ligand N3B and water molecules form N3B···H-O hydrogen bonds. As shown in Table S7, the N3B···H distance is drastically shortened from 2.47(3) Å to 1.77(3) Å after

light irradiation, which indicates a much stronger H-bond interaction in **1*$_{PES}$**. Fingerprint analysis for the intermolecular interactions confirmed the large variation in the N···H interaction (Figure S9). In parallel, the carbon atom of the cyanide ligand C3B interacts with the adjacent K3 cations. The heptacoordinated complex $[Mo(CN)_7]^{3-}$, the detached CN- anion, and the K3 cations are stacked in an alternating fashion in columns in the ac plane (Figure S4). This probably explains the significant increase in the *c* and *V* parameters in **1*$_{PES}$**. The superposition of the crystal structures of **1** and **1$_{relax}$** confirms the full reversibility (Figure S7b).

To complete these investigations, new CASPT2 calculations based on the crystal structure of **1*$_{PES}$** were conducted that confirmed the triplet nature of the ground state (Tables S2 and S3). Additionally, we recorded UV/Vis and IR spectra after 405 nm irradiation at 10 K (Figures S10 and S11). New transitions appear in the UV/Vis spectrum, one at about 310 nm and a second broad absorption in the visible region, which are consistent with the reflectivity data. TD-DFT calculations attribute the broad absorption band to an LMCT absorption from the detached cyanide to Mo. The IR spectrum reveals new features in the cyanide asymmetric stretching region (2040–2160 cm^{-1}) that can be assigned to the heptacoordinated $Mo(CN)_7$ complex and to the detached cyanide at 2080 cm^{-1}.[15] Further thermal annealing at 100 K gave back the UV/Vis and IR spectra recorded before irradiation, again supporting the full reversibility of the system.

Next, the photomagnetic properties of **1** were studied. As expected, the ground state of **1** is diamagnetic in agreement with two electrons paired in the lowest-energy d_{x2-y2} orbital in TDD geometry. When **1** was irradiated at 405 nm, the χT value gradually increases from zero to 0.37 $cm^3\ mol^{-1}$ K after 11 hours of irradiation (Figure S12). Then the light was switched off, and the low-temperature magnetizations and the temperature dependence of χT from 2 K to 200 K was measured (Figure 3). The non-superimposable reduced magnetizations suggest anisotropy in the photoinduced state. Again, complete relaxation was observed around 65 K, the

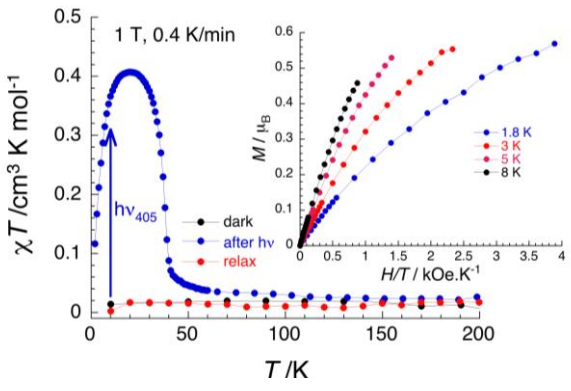

Figure 3. χT = f(T) plots of **1** measured in the dark (black circles), after 405 nm irradiation (blue circles) and after heating to 200 K (red circles). Inset: Reduced magnetizations at different temperatures in the photo-excited state.

temperature at which the compound returns to its diamagnetic state. Given the good agreement between the photocrystallographic analysis and the calculations, we consider that the observed properties are due to the population of a triplet state (S = 1). However, the obtained values (M_{sat} = 0.6 $N\mu_B$ at 1.8 K and χT_{max}= 0.4 $cm^3\ mol^{-1}$ K at 20 K) are far from what is expected for *S* = 1 (M_{sat} = 2 $N\mu_B$ and χT_{max}= 1 $cm^3\ mol^{-1}$ K assuming a Zeeman factor of 2). This can be explained by partial photoconversion, as observed in the photocrystallography study. Attempts to reproduce these magnetic data by including zero-field splitting parameters and partial conversion of the triplet state at 1.8–20 K (temper- ature range for which the thermal relaxation is negligible) failed or led to overparameterization.

In the literature, several examples of photoinduced magnetism with large structural reorganizations are mainly based on photoisomerization of the ligands linked to Fe^{II},[16] or reversible formation or rupture of metal–ligand (O or N) bonds in 3d metal ion (Ni^{II}, Fe^{II} and Fe^{III}) complexes.[17] In this study, we observed for the first time a photomagnetic effect based on light-induced bond cleavage in the solid state for a 4d metal complex. Our finding opens perspectives for the preparation of new cyanide complexes with interesting magnetic properties. As the first result in this direction, we have prepared the $[Mo^{IV}(CN)_7]^{3-}$ complex as the sole Mo based photoproduct using a photochemical synthetic pathway. $[K(crypt\text{-}222)]_3[Mo^{IV}(CN)_7]\cdot 3CH_3CN$ (**2**) has been crystallized from an acetonitrile solution containing the $[Mo(CN)_8]^{4-}$ anion in the presence of [2.2.2]cryptand after white light irradiation (see details in the Supporting Information). The crystal structure of **2** has been solved and shows a $[Mo^{IV}(CN)_7]^{3-}$ (an analog of $[W^{IV}(CN)_7]^{3-}$) [18] anion (Tables S8, S9 and Figures 4, S13, and S14). Analysis of the $[Mo(CN)_8]^{4-}$ coordination sphere revealed a pentagonal bipyramid with a CShM value of 0.26. The average Mo-C bond length is 2.172(6) Å, which is slightly longer than the ones found as 2.153(4) Å in **1*$_{PES}$**. The bond angle of Mo-C-N is more linear than in **1*$_{PES}$**. The magnetic properties of **2**

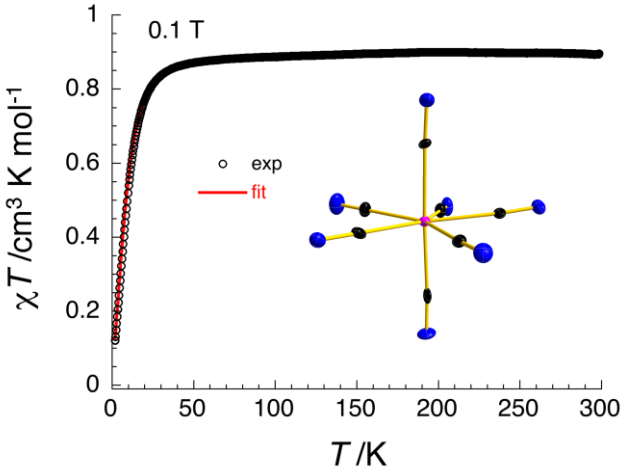

Figure 4. χT = f(T) plot of **2** measured at 0.1 T; the red line is the best fit to experimental data (see the main text for details). Inset: Molecular structure of the $[Mo^{IV}(CN)_7]^{3-}$ anion with thermal ellipsoids set at 30% probability.

(Figures 4 and S15) were studied and analyzed using the PHI software.[19] They are nicely reproduced with the following

parameters: g = 1.89(5), D = 20.6(1) cm^{-1},and E = -1.4(8) cm^{-1}. These parameters are comparable with the parameters obtained independently by theoretical calculations (Table S3; D = 33.0 cm^{-1} and g = 1.97).

In conclusion, we have shown that the photodissociation of a Mo-CN bond in **1** can be activated in the solid state at low temperature, or in solution at room temperature, and both ways allowed us to isolate an unprecedented $[Mo^{IV}(CN)_7]^{3-}$ complex with a triplet ground state with significant magnetic anisotropy. The perspectives of our work concern both future photophysical and photochemical studies. For instance, we are currently exploring the role of different cations in $[Mo^{IV}(CN)_8]^{4-}$ complex salts to evaluate their influence on the photophysical properties of the anion. Moreover, even if the photochemistry of the $[Mo^{IV}(CN)_8]^{4-}$ is well-documented, all of the known photoproducts are diamagnetic.[20] To the best of our knowledge, we have isolated the first paramagnetic photoproduct. This result opens very interesting perspectives in molecular magnetism for the photochemical preparation of new anisotropic building blocks.

Acknowledgements

X.Q. thanks the CSC for PhD funding. We thank Dr. Xiaoying Huang for assistance and fruitful discussions on crystal structure determination. Financial support from the CNRS (Pessac, Nancy, and Paris), the French PIA project “Lorraine Université d’Excellence”, reference ANR-15- IDEX-04-LUE, and the CPER is acknowledged. This work is supported by the Spanish ministry of economy and competition and EU-FEDER (CTQ2017-83566-P), and by the Generalitat de Catalunya (2017SGR629). C.dG. thanks Jean-Paul Malrieu for fruitful discussions over many years. Measurement time on the X-ray diffraction platform (PMD2X) of the Institut Jean Barriol is gratefully acknowledged. D.P. cordially acknowledges financial support from the Polish National Science Centre within the Sonata Bis 6 (2016/ 22/E/ST5/00055) and the COST Molspin project CA 15128.

Conflict of interest

The authors declare no conflict of interest.

Keywords: cyanides · magnetic properties · molybdenum · photochemistry · X-ray diffraction

How to cite: Angew. Chem. Int. Ed. 2020, 59, 3117–3121

Angew. Chem. 2020, 132, 3141–3145

[1] M. A. Halcrow, Spin-crossover Materials: Properties and Applications, Wiley, Hoboken, **2013**.
[2] D. Aguilà, Y. Prado, E. S. Koumousi, C. Mathonière, R. Clérac, *Chem. Soc. Rev.* **2016**, *45*, 203–224.
[3] J. M. Herrera, V. Marvaud, M. Verdaguer, J. Marrot, M. Kalisz, C. Mathonière, *Angew. Chem. Int. Ed.* **2004**, *43*, 5468–5471; *Angew. Chem.* **2004**, *116,* 5584–5587.
[4] a) N. Bridonneau, L. M. Chamoreau, G. Gontard, J. L. Cantin, J. von Bardeleben, V. Marvaud, *Dalton Trans.* **2016**, *45*, 9412– 9418; b) Y. Arimoto, S. I. Ohkoshi, Z. J. Zhong, H. Seino, Y. Mizobe, K. Hashimoto, *J. Am. Chem. Soc.* **2003**, *125*, 9240–9241; c) G. Rombaut, S. Golhen, L. Ouahab, C. Mathonière, O. Kahn, *J. Chem. Soc. Dalton Trans.* **2000**, 3609–3614; d) S. I. Ohkoshi, H.Tokoro, *Acc. Chem.Res.* **2012**, *45*, 1749–1758; e) N. Ozaki,H. Tokoro, Y. Hamada, A. Namai, T. Matsuda, S. Kaneko, S. I. Ohkoshi, *Adv. Funct. Mater.* **2012**, *22*, 2089–2093.
[5] S. I. Ohkoshi, H. Tokoro, T. Hozumi, Y. Zhang, K. Hashimoto, C. Mathonière I. Bord, G. Rombaut, M. Verelst, C. Cartier Dit Moulin, F. Villain, *J. Am. Chem. Soc.* **2006**, *128*, 270–277.
[6] a) M. Magott, M. Reczyński, B. Gaweł, B. Sieklucka, D. Pinkowicz, *J. Am. Chem. Soc.* **2018**, *140*, 15876–15882; b) M. Arczyński, J. Stanek, B. Sieklucka, K. R. Dunbar, D. Pinkowicz, *J. Am. Chem. Soc.* **2019**, *141*, 19067–19077.
[7] T. Yokoyama, K. Okamoto, T. Ohta, S.-i. Ohkoshi, K. Hashimoto, *Phys. Rev. B* **2002**, *65*, 064438.
[8] a) S. Brossard, F. Volatron, L. Lisnard, M. A. Arrio, L. Catala, C. Mathonière, T. Mallah, C. C. dit Moulin,A. Rogalev, F. Wilhelm, A. Smekhova, P. Sainctavit, *J. Am. Chem. Soc.* **2012**, *134*, 222– 228; b) M.-A. Arrio, J. Long, C. Cartier dit Moulin, A. Bach- schmidt, V. Marvaud, A. Rogalev, C. Mathonière, F. Wilhelm, P. Sainctavit, *J. Phys. Chem. C* **2010**, *114*, 593–600; c) M. A. Carvajal, M. Reguero, C. de Graaf, *Chem. Commun.* **2010**, *46*, 5737–5739; d) M. A. Carvajal, R. Caballol, C. de Graaf, *Dalton Trans.* **2011**, *40*, 7295–7303.
[9] N. Bridonneau, J. Long, J. L. Cantin, J. Von Bardeleben, S. Pillet, E. E. Bendeif, D. Aravena, E. Ruiz, V. Marvaud, *Chem. Commun.* **2015**, *51*, 8229–8232.
[10] M. Magott, O. Stefanczyk, B. Sieklucka, D. Pinkowicz, *Angew. Chem. Int. Ed.* **2017**, *56*, 13283–13287; *Angew. Chem.* **2017**, *129*, 13468–13472.
[11] J. Szklarzewicz, D. Matoga, K. Lewiński, *Inorg. Chim. Acta* **2007**, *360*, 2002–2008.
[12] R. Maurice, R. Bastardis, C. de Graaf, N. Suaud, T. Mallah, N. Guihery, *J. Chem. Theory Comput.* **2009**, *5*, 2977–2984.
[13] M. F. A. Hendrickx, V. S. Mironov, L. F. Chibotaru, A. Ceulemans, *Inorg. Chem.* **2004**, *43*, 3142–3150.
[14] M. Llunell, D. Casanova, J. Cirera, M. Alemany, S. Alvarez, SHAPE, v. 2.0, University of Barcelona, Barcelona, Spain, **2010**.
[15] R. A. Penneman, L. H. Jones, *J. Chem. Phys.* **1956**, *24*, 293–296.
[16] a) J. Zarembowitch, C. Roux, M.-L. Boillot, R. Claude, J.-P. Itie, A. Polian, M. Bolte, *Mol. Cryst. Liq. Cryst. Sci. Technol. Sect. A* **1993**, *234*, 247–254; b) B. Brachňaková, I. Šalitroš, *Chem. Pap.* **2018**, *72*, 773–798.
[17] a) S. M. Nelson, P. D. McIlroy, C. S. Stevenson, E. Kçnig, G. Ritter, J. Waigel, *J. Chem. Soc. Dalton Trans.* **1986**, 991–995; b) P. Guionneau, F. Le Gac, A. Kaiba, J. S. Costa, D. Chasseau, J. F. Létard, *Chem. Commun.* **2007**, 3723–3725; c) D. Aguilà, P. Dechambenoit, M. Rouzières, C. Mathonière, R. Clérac, *Chem. Commun.* **2017**, *53*, 11588–11591; d) S. Venkataramani, U. Jana, M. Dommaschk, F. D. Sonnichsen, F. Tuczek, R. Herges, *Science* **2011**, *331*, 445–448; e) S. Shankar, M. Peters, K. Steinborn, B. Krahwinkel, F. D. Sonnichsen, D. Grote, W. Sander, T. Lohmil- ler, O. Rudiger, R. Herges, *Nat. Commun.* **2018**, *9*, 4750; f) M. K. Peters, S. Hamer, T. Jakel, F. Rohricht, F. D. Sonnichsen, C. von Essen, M. Lahtinen, C. Naether, K. Rissanen, R. Herges, *Inorg. Chem.* **2019**, *58*, 5265–5272; g) Z.-Z. Gu, O. Sato, T. Iyoda, K. Hashimoto, A. Fujishima, *Chem. Mater.* **1997**, *9*, 1092– 1097; h) C. F. Sheu, C. H. Shih, K. Sugimoto, B. M. Cheng, M. Takata, Y. Wang, *Chem. Commun.* **2012**, *48*, 5715–5717; i) H. Petzold, P. Djomgoue, G. Horner, C. Lochenie, B. Weber, T. Ruffer, *Dalton Trans.* **2018**, *47*, 491–506; j) H. Petzold, P. Djomgoue, G. Hçrner, S. Heider, C. Lochenie, B. Weber, T. Rüffer, D. Schaarschmidt, *Dalton Trans.* **2017**, *46*, 6218–6229.
[18] F. J. Birk, D. Pinkowicz, K. R. Dunbar, *Angew. Chem. Int. Ed.* **2016**, *55*, 11368–11371; *Angew. Chem.* **2016**, *128*, 11540–11543.
[19] N. F. Chilton, R. P. Anderson, L. D. Turner, A. Soncini, K. S. Murray, *J. Comput. Chem.* **2013**, *34*, 1164–1175.
[20] a) J. Szklarzewicz, D. Matoga, A. Niezgoda, D. Yoshioka, M. Mikuriya, *Inorg. Chem.* **2007**, *46*, 9531–9533; b) J. Szklarzewicz, D. Matoga, A. Kłys , W. Łasocha, *Inorg. Chem.* **2008**, *47*, 5464– 5472.
[21] CCDC 1914245 (**1**), 1914246 (**1***), 1914247 (**1$_{relax}$**), and 1915471 (**2**) contain the supplementary crystallographic data for this paper. These data are provided free of charge by The Cambridge Crystallographic Data Centre.

COMMUNICATION

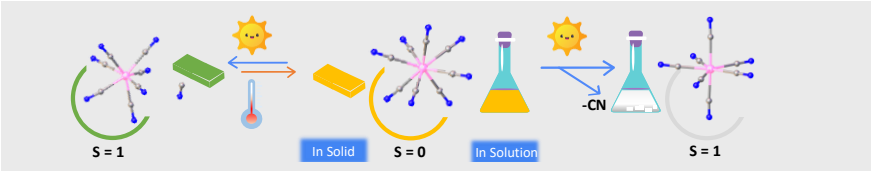

The crystal structure of $K_4Mo(CN)_8 \cdot 2H_2O$ collected at 10 K after a blue light irradiation reveals a light-induced breaking of one Mo-CN bond from the initial octacoordinated complex, concomitant with the photo-induced formation of a paramagnetic signal.

Xinghui Qi, Sébastien Pillet, Coen de Graaf, Michał Magott, El-Eulmi Bendeif, Philippe Guionneau, Mathieu Rouzières, Valérie Marvaud, Olaf Stefańczyk, Dawid Pinkowicz, Corine Mathonière**

Page No. – Page No.

Photoinduced Mo-CN Bond Breakage in Octacyanomolybdate Leading to Spin Triplet Trapping